IOP PUBLISHING JOURNAL OF PHYSICS: CONDENSED MATTER

J. Phys.: Condens. Matter **24** (2012) 385301 (5pp) doi:10.1088/0953-8984/24/38/385301

# Electron dephasing of a GaAs/AlGaAs quantum well with self-assembled InAs dots

**L Li[1], J Wang[1], Gil-Ho Kim[1] and D A Ritchie[2]**

[1] School of Electronic and Electrical Engineering and Sungkyunkwan University Advanced Institute of Nanotechnology, Sungkyunkwan University, Suwon 440-746, Republic of Korea
[2] Cavendish Laboratory, University of Cambridge, J J Thomson Avenue, Cambridge CB3 0HE, UK

E-mail: ghkim@skku.edu

Received 18 May 2012, in final form 24 July 2012
Published 3 September 2012
Online at stacks.iop.org/JPhysCM/24/385301

**Abstract**
We study the magnetotransport of a GaAs/AlGaAs quantum well with self-assembled InAs quantum dots. Negative magnetoresistance is observed at low field and analysed by weak localization theory. The temperature dependence of the extracted dephasing rate is linear, which shows that the inelastic electron–electron scattering processes with small energy transfer are the dominant contribution in breaking the electron phase coherence. The results are compared with those of a reference sample that contains no quantum dots.

(Some figures may appear in colour only in the online journal)

In recent years, self-assembled quantum dots have attracted the attention of researchers for application in optoelectronics and quantum computing. When inserted into a two-dimensional (2D) electron system the quantum dots form random repulsive scattering centres and reshape the scattering potential from ionized donors [1, 2]. It has been reported that variable range hopping of electrons can take place when applying a large negative gate voltage [3], and Landau quantization and localization can coexist in this system [4].

In this work we study the weak localization (WL) effect of a sample (D1) with embedded quantum dots by applying a modest positive gate voltage and compare it with the results from a reference sample (N1) in which, apart from the absence of the dots, all other conditions, such as wafer growth sequence and sample geometry, are the same. WL has been studied in various 2D GaAs systems [5–8]; and in a previous paper concerning the electron transport properties of the 2D gas with embedded InAs dots, WL features had been observed, but no detailed analysis was presented [11]. The WL effect originates from the enhanced backscattering probability due to quantum interference in a weakly disordered system. The application of a magnetic field introduces a phase difference for interfering electrons and thus suppresses the WL effect. Study of WL is very useful in understanding the scattering processes accounting for electron dephasing. These processes can be inelastic electron–electron/electron–phonon scattering, or scattering from magnetic impurities.

The 2D electron structures investigated contain a quantum well of 20 nm width formed in GaAs/AlGaAs heterostructures grown by molecular beam epitaxy (MBE). The quantum well is modulation-doped on one side with a 40 nm width spacer layer. For sample D1, self-assembled InAs dots are introduced [12] in the middle of the quantum well. The average spacing of the dots is approximately 50 nm and the majority of dots have an average diameter of 28 nm.

The samples were made by photo-lithography into a Hall bar pattern with a top gate to control the 2D electron density. Experiments were performed in a dilution fridge with a four-terminal low-frequency lock-in technique at temperatures from 200 mK to 1.0 K. Extra care was taken to ensure the actual sample temperature was identical to that recorded from the temperature sensor. The sample parameters are presented in table 1.

Data from sample D1 were obtained at gate voltage $V_g = 0$ and a small positive $V_g$, which correspond to electron densities of $n = 1.26 \times 10^{11}$ cm$^{-2}$ and $1.69 \times 10^{11}$ cm$^{-2}$, respectively. Figures 1(a) and (b) show that at

 © 2012 IOP Publishing Ltd Printed in the UK & the USA

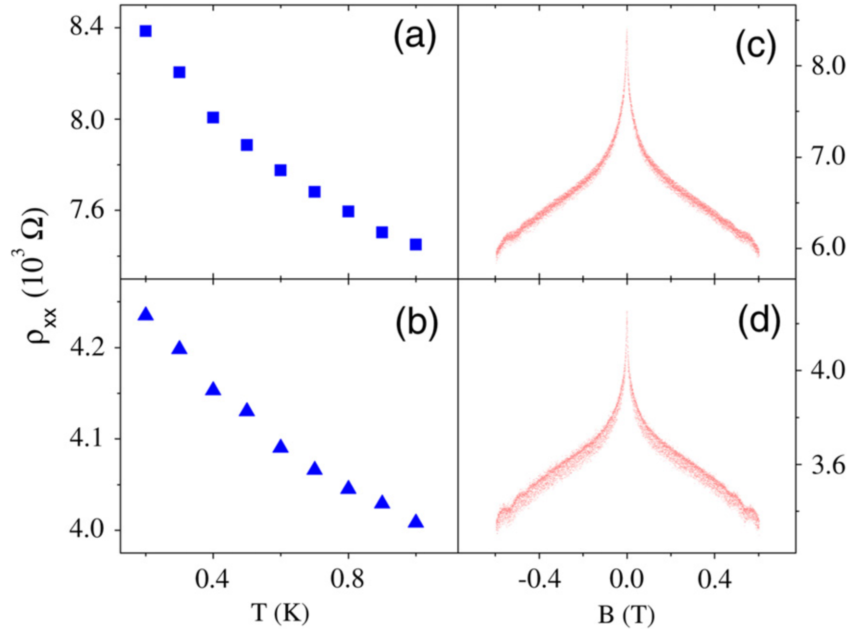


**Figure 1.** Temperature-dependent resistivity of D1 at $B = 0$ ((a), (b)); and magnetoresistivity measured at $T = 200$ mK ((c), (d)). Electron densities are $1.26 \times 10^{11}$ cm$^{-2}$ ((a), (c)), and $1.69 \times 10^{11}$ cm$^{-2}$ ((b), (d)).

**Table 1.** Parameters of sample D1 and sample N1.

| | $n$ ($10^{11}$ cm$^{-2}$) | $\mu$ (m$^2$ V$^{-1}$ s$^{-1}$) | $k_F l$ | $k_B T\tau/\hbar$ |
|---|---|---|---|---|
| D1 | 1.26 | 1.01 | 5.3 | 0.009–0.04 |
| D1 | 1.69 | 1.19 | 8.3 | 0.01–0.05 |
| N1 | 1.08 | 8.47 | 37 | 0.08–0.4 |
| N1 | 0.56 | 3.10 | 7.2 | 0.03–0.1 |

zero magnetic field, longitudinal resistivity increases with decreasing temperature. Figures 1(c) and (d) show the MR measured at 200 mK. It can be seen that at very low field the MR decreases sharply with increasing $B$, at larger field it shows a parabolic shape. This low-field sharply changing MR is caused by the WL effect, which is the focus of this work. The parabolic MR results from electron–electron interaction (EEI) [13, 14] corrections.

To apply the WL theory, we need to consider the parabolic background of the MR. Another important issue is to determine the Drude value of conductivity $\sigma_0$, which is essential in the calculation of the momentum scattering time $\tau$ and the transport field $B_{tr} = \hbar/4De\tau$, where $D$ is the diffusion constant. These are important parameters in the theoretical expression for WL.

When the WL is suppressed by a magnetic field and disappears, EEI becomes dominant in the MR, which is expressed by [15]

$$\rho_{xx} = \frac{1}{\sigma_0} - \frac{\delta\sigma_{xx}^{ee}(T)}{\sigma_0^2} + \frac{B^2\delta\sigma_{xx}^{ee}(T)}{(en)^2}, \quad (1)$$

where $\delta\sigma_{xx}^{ee}(T)$ is the EEI correction to conductivity. We plotted the MR as a function of $B^2$ to obtain the linear fit of the curve in the region where WL correction is not present. The intercept of the linear fit is dependent on temperature, because of the second term, i.e., the temperature-dependent EEI correction $\delta\sigma_{xx}^{ee}(T)$, in equation (1). To determine $\sigma_0$, we first find out the value of $\delta\sigma_{xx}^{ee}(T)$ from the slope, $\frac{\delta\sigma_{xx}^{ee}(T)}{(en)^2}$, of the plot. The intercept and the first two terms in equation (1) form a quadratic equation from which $\sigma_0$ was obtained. In this analysis the error in $\sigma_0$ for the highest and lowest temperatures is within 2%. As EEI may have a contribution to the Hall resistivity, and this contribution is more obvious at lower temperatures, in the analysis we used parameter values calculated from 1.0 K data. The mobility $\mu$ of D1 at the two studied electron densities is $1.01 \times 10^4$ cm$^2$ V$^{-1}$ s$^{-1}$ and $1.19 \times 10^4$ cm$^2$ V$^{-1}$ s$^{-1}$, the corresponding momentum relaxation time $\tau$ is $3.85 \times 10^{-13}$ s and $4.53 \times 10^{-13}$ s, respectively.

The WL theory is derived on the condition that $k_F l \gg 1$, where $k_F$ is the Fermi wave number and $l$ the mean free path. The values of $k_F l$ of D1 calculated from $\rho_0 = \frac{1}{\sigma_0} = \frac{h}{e^2}\frac{1}{k_F l}$ are 5.3 and 8.3, see table 1. These values are close to the range ($k_F l \simeq 2$–5) where the WL theory is not expected to be well applied. However it has been argued that the WL formula with a reduction prefactor can still be used to fit the MR in these regimes [7].

Figure 2 shows the conductivity of D1 calculated from the measured value of resistivity $\rho_{xx}$ and $\rho_{xy}$, $\sigma = \frac{\rho_{xx}}{\rho_{xx}^2+\rho_{xy}^2}$, as well as that calculated from the extracted parabolic shape MR $\rho_{para}$ and the measured value of $\rho_{xy}$, $\sigma = \frac{\rho_{para}}{\rho_{para}^2+\rho_{xy}^2}$. The WL correction to conductivity is found by comparing these two terms. The results were fitted with the equation [7, 16]

$$\delta\sigma = \frac{e^2}{\pi h(1+\gamma)^2}\alpha \times \left[\psi\left(\frac{1}{2}+\frac{\gamma}{b}\right) - \psi\left(\frac{1}{2}+\frac{1}{b}\right) - \ln\gamma\right], \quad (2)$$

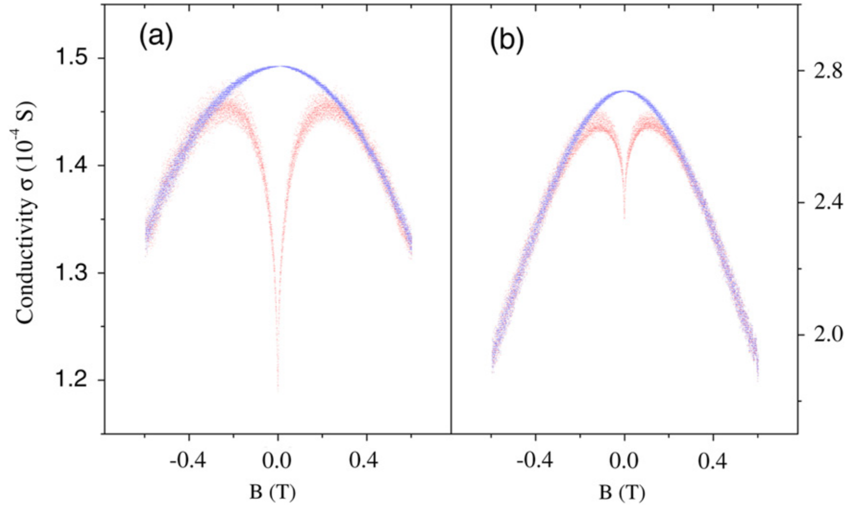


**Figure 2.** Conductivity of sample D1 obtained from experiments (red colour) and from calculation with parabolic MR $\rho_{para}$ (blue colour). The difference gives the WL correction of conductivity. $T = 200$ mK. (a) $n = 1.26 \times 10^{11}$ cm$^{-2}$; (b) $n = 1.69 \times 10^{11}$ cm$^{-2}$.

where $\gamma = \tau/\tau_\varphi$, $\tau_\varphi$ is the dephasing time, $\psi(x)$ is the digamma function, and $b = \frac{1}{1+\gamma^2}\frac{B}{B_{tr}}$. $\alpha$ is the reduction prefactor, which should be unity as per the conventional WL theory. Results are better fitted with $\alpha < 1$ when the conductivity is not significantly larger than $\frac{2h}{e^2}$ [7, 8]. For non-interacting electrons $\alpha$ is independent of temperature and can be expressed as

$$\alpha \simeq 1 - \frac{e^2}{\pi h \sigma_0} = 1 - \frac{1}{\pi k_F l}. \tag{3}$$

In the fitting process, for a specific electron density we first varied $\gamma$ as well as $\alpha$ to obtain the best fit at the lowest temperature. Then, $\alpha$ was fixed for this electron density and only $\gamma$ was treated as a variable to fit the data at various remaining temperatures. Figure 3 shows the results of the WL correction at selected temperatures. The fitting results for $\alpha$ were found to be 0.54 and 0.62, which are significantly smaller than the value (0.94 and 0.96 respectively) predicted by equation (3), but are close to that ($\alpha = 0.61$) from [9] in a Si/SiGe quantum well with similar conductivity. Our results show that for a specific electron density $\alpha$ does not depend on temperature, which is in agreement with previous experiments [9, 10]. $\gamma$ varies from 0.0048 to 0.015. The dephasing lengths, $l_\varphi = (D\tau_\varphi)^{1/2}$, are found too lie in the range from 320 to 850 nm. These lengths are much larger than the average spacing between the quantum dots. We estimated that an electron passes through 6–17 dot sites before losing its phase coherence. InAs dots are negatively charged and scattering from these dots is elastic. This elastic scattering process can effectively cause momentum transfer processes to take place, but it does not make a direct contribution in breaking the electron phase coherence, which is determined by inelastic scattering processes.

It is believed that in the temperature range applied in this study, the contribution from the electron–phonon scattering to the dephasing rate is negligible [6, 17]. This implies that the electron–electron scattering processes are

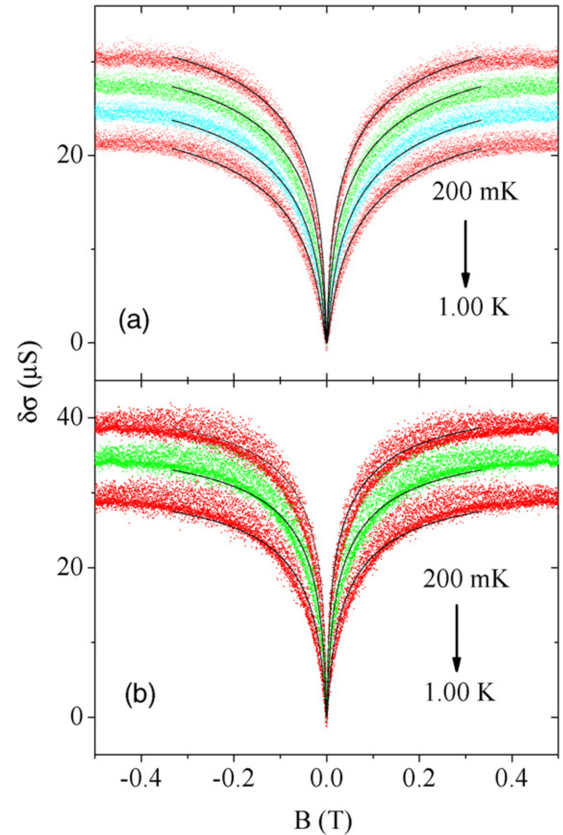


**Figure 3.** WL correction of conductivity for D1 as a function of magnetic field. Coloured symbols represent experimental results, solid curves are fits to equation (2). (a) $n = 1.26 \times 10^{11}$ cm$^{-2}$ at $T = 200$, 400, 700 mK, and 1.00 K. (b) $n = 1.69 \times 10^{11}$ cm$^{-2}$ at $T = 200$, 500 mK, and 1.00 K.

dominant in the dephasing mechanism. According to the WL theory, depending on the value of $k_B T\tau/\hbar$, where $k_B$ is the Boltzmann constant, the temperature dependence of the dephasing rate caused by electron–electron scattering is

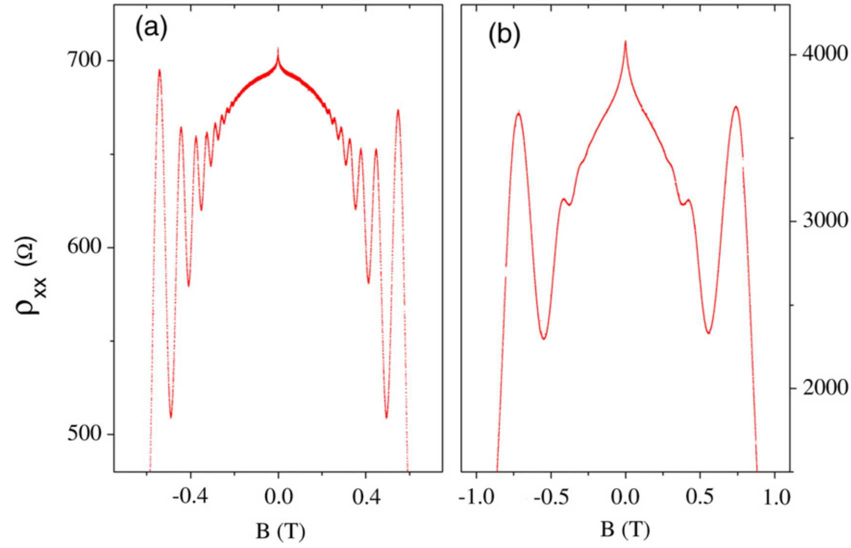


**Figure 4.** Magnetoresistivity of sample N1 measured at $T = 200$ mK. (a) $n = 1.08 \times 10^{11}$ cm$^{-2}$; (b) $n = 5.6 \times 10^{10}$ cm$^{-2}$.

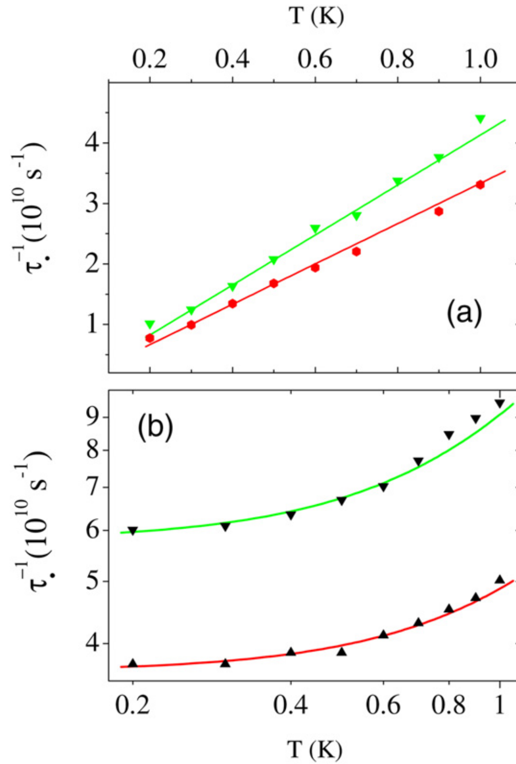


**Figure 5.** (a) Dephasing rate as a function of temperature for sample D1. Symbols denote experimental results; lines are calculated from equation (4). Upper curve: $n = 1.26 \times 10^{11}$ cm$^{-2}$; Lower curve: $n = 1.69 \times 10^{11}$ cm$^{-2}$. (b) Dephasing rate of the reference sample N1 in double logarithm scale. Upper curve: $5.6 \times 10^{10}$ cm$^{-2}$; lower curve: $n = 1.08 \times 10^{11}$ cm$^{-2}$. Lines are calculations by equation (3) from [6] with prefactors 0.82 and 1.3 for the high and low electron densities, respectively. The saturation values are $3.62 \times 10^{10}$ and $5.79 \times 10^{10}$ s$^{-1}$.

linear when $k_B T\tau/\hbar \ll 1$, or quadratic when $k_B T\tau/\hbar \gg 1$. The quadratic temperature dependence is attributed to the collisions with large momentum transfer in a clean electron system (i.e., free of disorder) while the linear temperature dependence is ascribed to processes with small energy transfer in a disordered conductor. The value of $k_B T\tau/\hbar$ for D1 varies from 0.009 to 0.05. We compare our experimental results with the theoretical prediction of the dephasing rate in the diffusive regime ($k_B T\tau/\hbar \ll 1$) [6, 18],

$$\tau_\varphi^{-1}(T) = \frac{k_B T}{2E_F\tau} \ln\left(\frac{2E_F\tau}{\hbar}\right). \tag{4}$$

Here $E_F = \pi\hbar^2 n/m^*$ is the Fermi energy, $m^*$ is the effective mass of the carriers. We can see from figure 5(a) that in the entire temperature range, the dephasing rates extracted from the fitting of MR agree well with the theoretical value. We also did MR measurements (figure 4) with the reference sample N1, which show low electron density, but higher mobility. For N1 the measurements were done with zero and a negative $V_g$. There is no reduction prefactor when doing the fit by equation (2), i.e., $\alpha = 1$. This is interesting since we can see from table 1 that the value $k_F l$ for N1 at $n = 1.08 \times 10^{11}$ cm$^{-2}$ is much larger, but at $n = 5.6 \times 10^{10}$ cm$^{-2}$ $k_F l$ is very close to that of D1 at $n = 1.69 \times 10^{11}$ cm$^{-2}$. The dephasing rates show a quadratic temperature dependence with saturation values, figure 5(b). Previous works had discussed the saturation effect by an additional dephasing mechanism caused by external non-equilibrium noise [6, 19]. In N1, the values of $k_B T\tau/\hbar$ are relatively larger than those of D1, but still significantly smaller than 1. We consider that the difference in dephasing mechanism can be traced to the different impurity scattering potentials in these samples. In N1, the impurity scattering comes from the ionized donors set back by a spacer layer. This scattering potential is long range. In D1, with the introduced InAs dots, the impurity scattering comes both from ionized donors in the doping layer and from quantum dots within the quantum well. Thus the potential is of mixed long-range and short-range type. In high-mobility low-density samples the dephasing rate tends to show quadratic temperature dependence [6]. When incorporated with dots the structure

acquires more diffusive features. In contrast with this work, a previous paper on electron dephasing in 2D GaAs structures with similar electron mobility showed that the temperature dependence of dephasing rate included both linear and quadratic terms [5], but without saturation values. A linear temperature dependence has been observed in a Si/SiGe quantum well [9] with slightly small mobility compared to sample D1, and in a GaAs/AlGaAs heterostructure [10] with similar electron density. Compared to our sample with 40 nm spacer layer, the samples used in [9, 10] have much smaller spacer layers (18 and 10 nm respectively). Existing results show that the temperature dependence of the dephasing rate is highly related to the mobility and structure of the sample.

In this work, we have carried out temperature-dependent MR measurements in a 2D electron system with self-assembled InAs quantum dots. It is found that at low magnetic fields the MR can be described by the WL theory with a reduction prefactor. The dephasing rate extracted from the MR exhibits a linear dependence on temperature, which is in agreement with the localization theory in a disordered conductor. We compared the results with those from a reference sample containing no dots and previous reports on 2D systems.

## Acknowledgments

This research was supported by the World Class University program through the National Research Foundation of Korea funded by the Ministry of Education, Science and Technology (Grant No. R32-10204).

## References

[1] Kannan E S, Kim G-H and Ritchie D A 2009 *Appl. Phys. Lett.* **95** 143506
[2] Ribeiro E, Muller E, Heinzel T, Auderset H, Ensslin K, Medeiros-Ribeiro G and Petroff P M 1998 *Phys. Rev.* B **58** 1506
[3] Li L, Kim G-H, Thomas K J and Ritchie D A 2011 *Phys. Rev.* B **83** 153304
[4] Kim G-H, Liang C-T, Huang C F, Nicholls J T, Ritchie D A, Kim P S, Oh C H, Juang J R and Chang Y H 2004 *Phys. Rev.* B **69** 073311
[5] Choi K K, Tsui D C and Alavi K 1987 *Phys. Rev.* B **36** 7751
[6] Proskuryakov Y Y, Savchenko A K, Safonov S S, Pepper M, Simmons M Y and Ritchie D A 2001 *Phys. Rev. Lett.* **86** 4895
[7] Minkov G M, Germanenko A V and Gornyi I V 2004 *Phys. Rev.* B **70** 245423
[8] Minkov G M, Germanenko A V, Rut O E, Sherstobitov A A and Zvonkov B N 2010 *Phys. Rev.* B **82** 035306
[9] Senz V, Heinzel T, Ihn T, Ensslin K, Dehlinger G, Grützmacher D and Gennser U 2000 *Phys. Rev.* B **61** 5082
[10] Lin B J F, Paalanen M A, Gossard A C and Tsui D C 1984 *Phys. Rev.* B **29** 927
[11] Heinzel T, Jaggi R, Ribeiro E, Waldkirch M V, Ensslin K, Ulloa S E, Medeiros-Ribeiro G and Petroff P M 2003 *Europhys. Lett.* **61** 674
[12] Kim G-H, Ritchie D A, Liang C-T, Lian G D, Yuan J, Pepper M and Brown L M 2001 *Appl. Phys. Lett.* **78** 3896
[13] Li L, Proskuryakov Y Y, Savchenko A K, Linfield E H and Ritchie D A 2003 *Phys. Rev. Lett.* **90** 076802
[14] Gornyi I V and Mirlin A D 2003 *Phys. Rev. Lett.* **90** 076801
[15] Beenakker C W J and von Houten H 1991 *Quantum Transport in Semiconductor Nanostructures* (*Solid States Physics* vol 44) ed H Ehrenreich and D Turnbull (New York: Academic) p 74
[16] Wittmann H-P and Schmid A 1987 *J. Low Temp. Phys.* **69** 131
[17] Karpus V 1990 *Semicond. Sci. Technol.* **5** 691
[18] Altshuler B L and Aronov A G 1985 *Electron–Electron Interaction in Disordered Systems* ed A L Efros and M Pollak (Amsterdam: North-Holland)
[19] Altshuler B L, Gershenson M E and Aleiner I L 1998 *Physica* E **3** 58